EcoHealth (© 2006)
DOI: 10.1007/s10393-006-0061-5

EcoHealth

© 2006 EcoHealth Journal Consortium

Original Contributions

Cholera Threat to Humans in Ghana Is Influenced by Both Global and Regional Climatic Variability

Guillaume Constantin de Magny,[1,2] Bernard Cazelles,[3] and Jean-François Guégan[1]

[1]*GEMI, UMR CNRS/IRD 2724, Centre IRD de Montpellier, Equipe "Evolution des Systèmes Symbiotiques," 911 avenue Agropolis, BP 64501, 34394 Montpellier cedex 05, France*
[2]*US ESPACE 140, IRD, 500 rue Jean-François Breton, 34093 Montpellier cedex 05, France*
[3]*CNRS-UMR 7625, Ecole Normale Supérieure, 46 rue d'Ulm, 75230 Paris cedex 05, France*

Abstract: Cholera, an acute diarrheal illness, is caused by infection of the intestine with the bacterium *Vibrio cholerae* after ingestion of contaminated water or food. The disease had disappeared from most of the developed countries in the last 50 years, but cholera epidemics remain a major public health problem in many developing countries, most often localized in tropical areas. Cholera is an infectious disease for which a relationship between disease temporal patterns and climate has been demonstrated, but only in an endemic context and for local areas of Asia and South America. Until now, similar studies have not been done in an epidemic context, on the African continent, although the largest number of cholera cases has been reported for those countries by the World Health Organization. The wavelet method was used in order to explore periodicity in (i) a long-time monthly cholera incidence in Ghana, West Africa, (ii) proxy environmental variables, and (iii) climatic indices time series, from 1975 to 1995. Cross-analysis were done to explore links between these time series, i.e., between cholera and climate. Results showed strong statistical association (coherency) from the end of the 1980s, between cholera outbreak resurgences in Ghana and the climatic/environmental parameters under scrutiny. Further examination of the existence of common spatial and temporal patterns in infectious diseases on the continent of Africa will permit development of more effective treatment of disease.

Key words: cholera, climate, Africa, communicable disease, statistical, disease outbreaks

Introduction

Cholera is an ancient disease which disappeared from most developed countries some 50 years ago. However, it continues to persist in many parts of the world, with serious epidemics often localized in tropical areas (World Health Organization, 2005). Despite improved hygiene in many of these countries, along with advances in diagnostic methods and the development of new drugs and vaccines by the second half of the 20th century, there has been an apparent increase in the emergence of many new and also some more ancient infectious diseases (Smith et al., 2005). Within this context, cholera is, at present, undoubtedly one of the most important of the resurgent diseases (UNEP, 2005). This highly contagious disease is caused by specific strains of the bacterium *Vibrio cholerae*, following ingestion of contami-

Correspondence to: Guillaume Constantin de Magny, e-mail: g.demagny@gmail.com

nated water or seafood (Kelley, 2001). *V. cholerae* is naturally present in the environment and is autochthonous to coastal and estuarine ecosystems (Xu, 1982). Because many phyto- and zooplankton organisms may serve as reservoirs for the cholera bacterium (Tamplin et al., 1990; Islam et al., 1994, 1999; Colwell, 1996), disease outbreaks in humans may be strongly correlated with the population and community dynamics of these hosts (Lobitz et al., 2000; Lipp et al., 2002; Colwell et al., 2003). Previous studies of cholera population dynamics have proposed links between climate, oceanographic environmental conditions such as temperature, phytoplankton productivity, cholera phage density in the aquatic environment, and human cases of cholera morbidity and mortality (Epstein, 1993; Colwell and Huq, 2001; Faruque et al., 2005). Climate may affect the dynamics of cholera by shifting pathogen or host reservoir species abundance, population dynamics, and community interactions (Bouma and Pascual, 2001; Pascual et al., 2002; Koelle et al., 2005a). For example, cholera outbreaks in Peru and Bangladesh have been linked to periodic climatic cycles such as the El Niño Southern Oscillation (*ENSO*) (Salazar-Lindo et al., 1997; Pascual et al., 2000; Rodo et al., 2002). In particular, variations in rainfall in the Indian Ocean during the monsoon may induce predictable variations in phyto- and zooplankton abundance in the marine environment, which appears to be correlated with the appearance of cholera cases in coastal human communities (Colwell, 1996; Faruque et al., 2005). Floods and droughts may affect not only the concentration of the bacterium in the environment, but its survival, through the effect exerted by these environmental changes on salinity, sunlight, pH, and nutrient concentrations (Piarroux and Bompangue, 2006; Miller et al., 1982; Islam et al., 1990; Colwell, 1996; Montilla et al., 1996; Bouma and Pascual, 2001). It is also likely that many other factors, such as the level of poverty and human density, may influence the spatial and temporal distribution of cholera cases (Faruque et al., 1998, 2005; Ali et al., 2002). But perhaps now more than ever, cholera dynamics is found to be strongly associated with climate and seasonal variability (Colwell, 1996; Bouma and Pascual, 2001; Colwell and Huq, 2001; Pascual et al., 2002; Koelle et al., 2005a). Based on quantitative empirical studies, relationships have been shown to exist between cholera epidemics, land and sea surface temperature anomalies (*LSTAs*), rainfall, and *ENSO*, with the latter parameter quantified by the Southern Oscillation Index (*SOI*), for the Asian and South American subcontinents (Checkley et al., 2000; Pascual et al., 2000, 2002; Speelmon et al., 2000; Bouma and Pascual, 2001; Simanjuntak et al., 2001; Rodo et al., 2002; Koelle et al., 2005b). In particular, an increased role of interannual climate variability in cholera interannual dynamics in Bangladesh has been suggested, with a strong and consistent signature of *ENSO*, at least for certain time periods (Rodo et al., 2002). All these findings in an epidemiological endemic context, suggest that certain aspects of climate are associated with human cholera incidence in specific areas of the intertropical belt, i.e., Peru and Bangladesh. Until now, no such study has been performed in an epidemic context, in Africa, although the greatest number of cases (more than 95,000 in 2004) have been reported (World Health Organization, 2005).

Our objective was to determine whether an association between environmental factors and cholera outbreaks, might explain temporal patterns of the cholera incidence observed in Ghana, a country on the African tropical Atlantic Coast (Gulf of Guinea). We first used wavelet analyses to explain temporal patterns of cholera incidence in Ghana, and climatic signals at both a global, i.e., *SOI* and Indian Ocean Index (*IOI*) and regional scales, i.e., *LSTAs* and rainfall over the past 20 years. Classical times series methods can only be used for stationary time series (in which the statistical properties do not vary in time), but epidemiological or climatic time series are typically noisy, complex, and nonstationary. The main advantage of this method consists in the detection of periodicity evolution in time. Secondly, with the wavelet coherence method, we examined pairwise associations by crossing all temporal time series with each other in order to guide our hypotheses regarding correlations between cholera and climate. Finally, we explored the existence of synchrony and phase delays in the time series under scrutiny in order to quantify these phenomena.

Materials and Methods

Epidemiological Data

The numbers of cholera cases used in this study represent reports of morbidity cases in Ghana for the years 1975 to 1995, compiled by the *Weekly Epidemiological* Record published by the World Health Organization (WHO), available at the WHO website (http://www.who.int/wer/en/), and computerized on a personal database (Access format). Since the periods between two reports are not uniform, we chose to transform the data by linear interpolation in order to obtain monthly data. This involved 47 of the overall 135 notifications. When the period of WHO

notification was longer than a month, or began one month and finished the following month or later, e.g., March 15–April 24, 1976, we proportionally attributed the number of notification cases over the total period (March 15–April 24), based on the number of days in each of the respective months, i.e., 17 days in March and 24 days in April, during that total period.

Climatic and Environmental Data

The Southern Oscillation Index (*SOI*) is defined as the monthly standardized sea-level atmospheric pressure (*SLP*) anomaly between the eastern Pacific, Tahiti (20°S, 150°W), and the western Pacific, Darwin (10°S, 130°E), from 1975 to 1995; data are available on the Climate Prediction Center website (http://www.cpc.ncep.noaa.gov/data/indices/soi).

The Indian Ocean Index (*IOI*) (Marsac and Le Blanc, 1998) is based on the variability in *SLP* between the West Indian Ocean, the Seychelles (4°S, 55°E) and the East Indian Ocean, Darwin (10°S, 130°E), and is elaborated by computing the differences between the monthly standardized anomalies of *SLP* at both sites (Mahe minus Darwin). *IOI* warm events (increase in the sea surface temperature and strengthening of easterly winds at the equator) are associated with *IOI* values less than −1. In contrast, values greater than +1 indicate cold events (Marsac, 2001). This *IOI* index adapted to the Indian Ocean is significantly correlated with the *SOI* ($r = 0.52$, $P < 0.001$, two sided, for the period 1975–1995).

Monthly *LSTAs* data for the period from 1975 to 1995 were extracted from the Global Ocean Surface Temperature Atlas (GOSTAplus) for a grid of pixels of 5° square in latitude and longitude. Data were available on the NASA Physical Oceanography Distributed Active Archive Center website (http://www.podaac.jpl.nasa.gov/). Unfortunately, data were unavailable after 1995. Data were extracted from two selected pixels (see Fig. 1) centered at 2.50°W–7.50°N to represent the regional land surface temperature anomaly (hereafter called *LSTA1*), and 2.50°W–2.50°N to represent the regional sea surface temperature anomalies along the coast (hereafter called *LSTA2*).

Rainfall data were extracted from a historical monthly precipitation data set from 1975 to 1995, and are available on the Climate Research unit website (http://www.cru.uea.ac.uk/~mikeh/datasets/global/) of the University of East Anglia at Norwich, UK. They correspond to monthly data for a grid of pixels at a resolution of 2.5 degrees of latitude and 3.75 degrees of longitude. For our purposes, we choose to extract the rainfall data of one precise zone for which information was homogenous, and that was centered at 0.00°E in longitude and 7.50°N in latitude (see Fig. 1). We opted for this specific zone since it is the most representative area of human community settlements in Ghana, with most of the country's population concentrated near the coastline. Note here that data resolution for the two data sets, i.e., *LSTA* and rainfall, are not defined according to the same spatial scale resolution.

Wavelet Analysis of Both Univariate and Bivariate Time Series

With nonstationary population time series, as observed in many biological systems (Torrence and Compo, 1998), Fourier analysis used to analyze the relationship between oscillating time series (Chatfield, 2004) is not appropriate because it cannot take into account the often-observed drifts or changes in the main periodic components of such series. Wavelet analyses (Torrence and Compo, 1998; Grenfell et al., 2001) are well suited to biological time series, as they enable exploration of local variations in frequency and periodicity in time, as well as indicating the temporal trend of these periodic components through time (Torrence and Compo, 1998). Over the past 5 years, wavelet analysis has become a mathematical tool that has been used in epidemiology for exploring spatial and temporal dynamics of disease (Grenfell et al., 2001; Broutin et al., 2005; Cazelles et al., 2005). It is particularly well suited to the context of our study, since it may help to determine whether periodic components of disease time series are present over the total time series. For more technical details on wavelet analysis, see the work by Broutin et al. (2005).

In this work, prior to wavelet analyses, the disease incidence time series was square-root-transformed, a standard procedure used in wavelet analysis to dampen extremes in variability. In addition, we extracted all oscillating components of rainfall and *LSTAs* time series with a period of less than 12 months using a low-pass Gaussian filter to deseasonalize the data; all the series were normalized.

Coherency and Synchrony Analyses

In order to quantify the statistical association between two times series, we employed the technique of wavelet coherency (Broutin et al., 2005; Cazelles et al., 2005). Wavelet

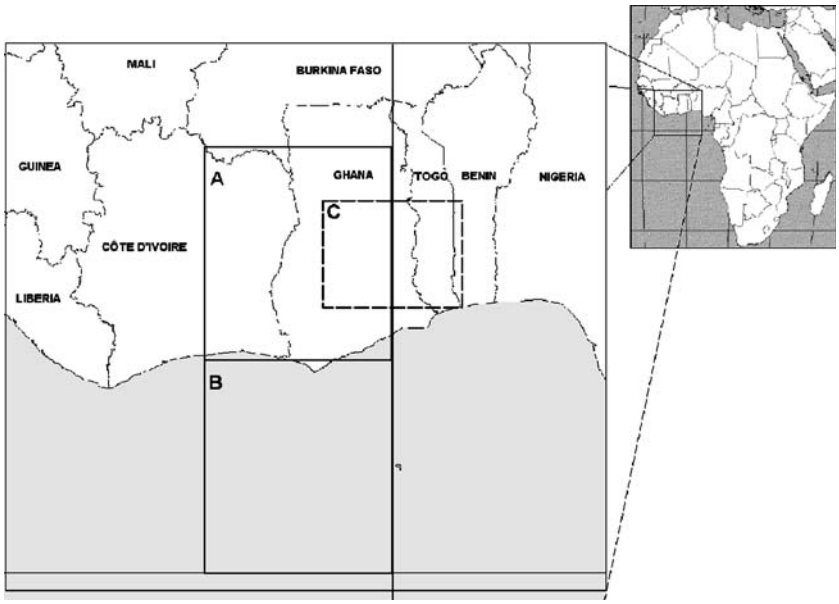

Figure 1. Ghana shown on a map of West African countries. The two contiguous black line squares represent the two areas selected for analysis of land (**A**: *LSTA1*) and sea (**B**: *LSTA2*) surface temperature anomaly time series. The black dashed line square (**C**) is the selected area for monthly rainfall time series.

coherency identifies the possibility that two independent time series, e.g., disease time series and SST, will correlate with one another. Coherency is roughly similar to classical correlation, but it pertains to the oscillating components in a given frequency mode. This tool allows us to quantify whether or not two time series tend to oscillate simultaneously, rising and falling together with the same period (Cazelles and Stone 2003; Broutin et al., 2005). To add to coherence analysis, we computed the oscillating components in a given frequency mode, the time lag between two oscillating components, and then the mean time lag (*MeanTL*). For more technical details on coherency and synchrony analysis, see the work by Broutin et al. (2005).

Results

Periodicity

All monthly time series data are represented in the left panel of Figure 2, and results from the local and averaged wavelet spectrum analyses are illustrated in the middle and right panels in the same figure, respectively.

For cholera incidence cases in Ghana, the wavelet power spectrum clearly showed the existence of two continuous cycles, an approximate 4–5-year cycle and an approximate 7–8-year cycle, during the entire time period. In the latter case, we are in the limits of statistical interpretation due to a too short length of the series. In addition, a 2–3-year cycle also appeared, but only during the period between 1988 and 1995 (Fig. 2A, middle and right). Wavelet analysis of *SOI* detected a significant 4–5-year periodic mode for the whole time series and a 2–3-year periodic mode from 1975 to 1991 (Fig. 2B, middle and right). For *IOI* in the 1975–1995 time period, results showed a significant 2–6-year mode, but the periodicity was transiently changing (Fig. 2C middle and right). Figure 2C, middle panel, shows an increasing periodicity of climate oscillations from 6 to 3 years occurring over the entire period of time, revealing those a progressive acceleration of the phenomenon. Wavelet analysis of deseasonalized rainfall displayed significant major 6-year periodicities (Fig. 2D, middle and right). Furthermore, a 2-year mode took place from 1986 to 1994 (Fig. 2D middle). The global wavelet power spectrums of land surface temperature anomalies are noticeably similar with both a 2–3-year and a major 7-year periodicities (Fig. 2E and F, middle and right). These periodicities changed over time, with a 2-year mode present for *LSTA1* from 1976 to 1986 and from 1990 to 1995, and a 3-year cycle from 1975 to 1992 (Fig. 2E, middle). For *LSTA2*, the 2-year mode was present from 1976 to 1984 and from 1992 to 1995, and a 3-year cycle took place from 1980 to 1992.

Coherence Analyses

Results for coherency and main oscillating components (left and right panels, respectively) are illustrated in Figure 3. Wavelet coherency of pairwise time series comparisons reveals only a discontinuous association between the different variables in the 2–3-year periodic band. For the

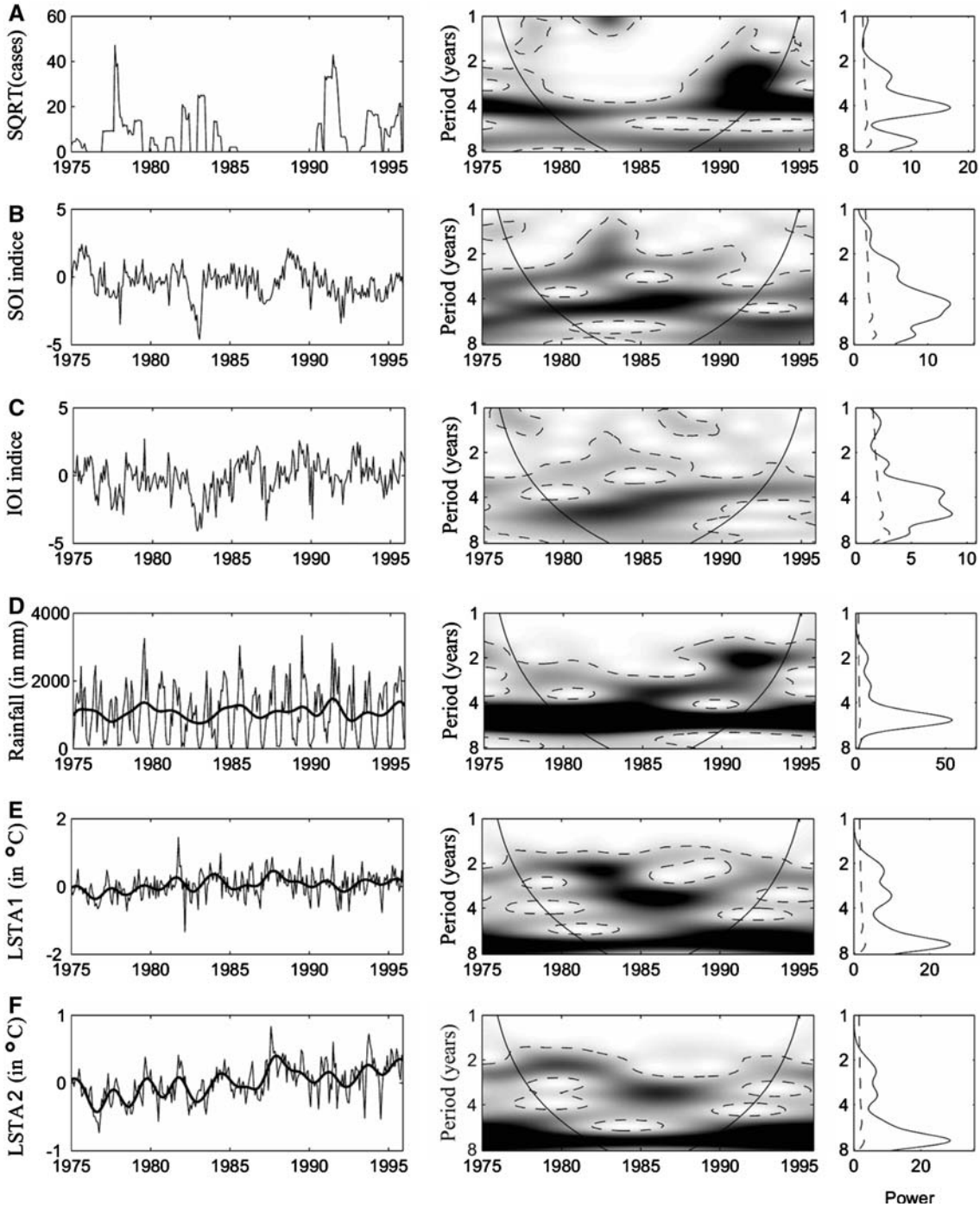

Figure 2. Wavelet analyses of epidemiological, environmental, and climatic time series for Ghana. **(A)** Square-root-transformed (*SQRT*) cholera cases; **(B)** Southern Oscillation Index (*SOI*); **(C)** Indian Ocean Index (*IOI*); **(D)** rainfall; **(E)** Land Surface Temperature Anomaly (*LSTA1*), 2.5°W–7.5°N; and **(F)** *LSTA2*, 2.5°W–2.5°N. For each time series, the left panel illustrates real data over time. The solid and dense lines correspond respectively to the uncut time series and the deseasonalized time series. The middle panel shows the wavelet power spectrum for the different series (x-axis: time in year; y-axis: period in year). The power is coded from low values, in white, to high values, in black. The black dashed lines show the $\alpha = 5\%$ significance level computed after 1000 bootstrapped series. The inside area within the cone of influence (black line) indicates the region not influenced by edge effects. The right panel corresponds to the average wavelet spectrum (black line) with its significant threshold value of 5% (dashed line).

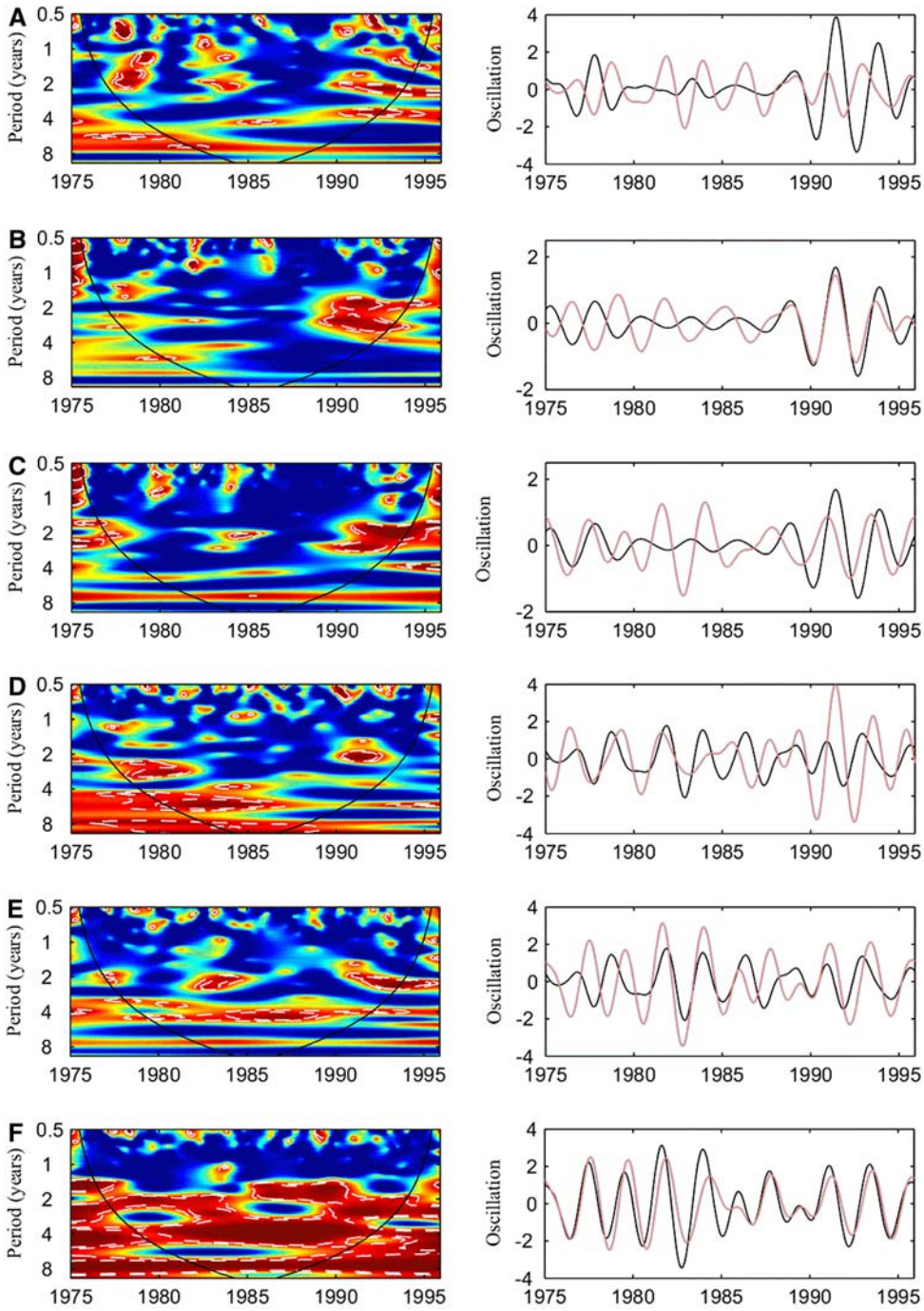

Figure 3. Wavelet coherency (using the Morlet wavelet function) and synchrony analyses of all studied time series for Ghana. (**A**) incidence/*IOI*; (**B**) incidence/rainfall; (**C**) incidence/*LSTA1*; (**D**) *IOI*/rainfall; (**E**) *IOI*/*LSTA1*; and (**F**) *LSTA1*/*LSTA2*. The left panel shows the wavelet coherency of different series (x-axis: time in year; y-axis: period in year). The power is coded from low values, in dark blue, to high values, in dark red. The white dashed lines show the $\alpha = 5\%$ significance level computed after 1000 bootstrapped series. The inside area within the cone of influence (black line) indicates the region not influenced by edge effects. Right panel shows oscillating components computed with the wavelet transform in the 2–3-year period band. Black lines: first variable; pale-orange line: second variable.

sake of brevity in the present work, coherency in the other periodic bands is not discussed. Interestingly, coherence analysis attested to a strong association between cholera incidence and *IOI* in the 2–3-year periodic band from 1989 to 1995 (Fig. 3A). Oscillating component analysis computed in the 2–3-year periodic band showed that *IOI*, with its maximum negative value in 1990, was in advance on disease incidence, with its maximum positive value in 1991 with a time delay of 16 months (Fig. 3A, right). Results of coherence reveals also the existence of strong associations between, (i) cholera case incidence and rainfall, and (ii) disease incidence and *LSTA1* time series. Both signals co-varied significantly with a 2–3-year periodicity from 1988 to 1995 (Fig. 3B and C, on the left). Therefore, oscillating components were computed in the 2–3-year periodic band, and it showed that cholera incidence and rainfall were synchronous from 1988 to 1992 (Fig. 3B, on the right). The mean time lag between the signals (incidence/rainfall) was

−0.75 (SD 0.56) months, and cholera incidence and *LSTA1* were not synchronous, with *LSTA1* being in advance of 5.7 (SD 0.15) months (Fig. 3C, on the right). The wavelet coherency between rainfall and *IOI* time series in the 2–3-year periodic band showed a strong association from 1989 to 1993 (Fig. 3D, on the left). The oscillatory components revealed that *IOI*, with its maximum negative value in 1990, was in advance of rainfall, reaching its maximum positive value in 1991 with a delay of 16 months (Fig. 3D, on the right). Coherency was highlighted between *IOI* and *LSTA1* in the 2–3-year periodic band from 1990 to 1995 (Fig. 3E, on the left), and the oscillation components showed that the negative phase of *IOI* (warm event) was in advance of 12 months for this period (Fig. 3E, on the right). The wavelet coherency between the *LSTAs* values showed strong coherency in the 1.5–8-year periodic band (Fig. 3F, on the left). The oscillatory components computed in the 2–3-year periodic band showed that from 1986 to 1992 the *LSTAs* series were more synchronous, with *LSTA1* being in advance by 1.54 (SD 0.22) months. The synchrony between the *LSTAs* series was less evident during the previous period from 1978 to 1988, with a delay of 3.33 (SD 1.45) months (Fig. 3F, on the right).

Discussion

Our findings clearly show the existence of an association between temporal patterns of cholera cases in Ghana at the end of the 1980s, with both the global climatic index (e.g., *IOI*) and two regional climatic parameters, i.e., land and/or sea surface temperature anomalies, and rainfall. To our knowledge, this study is the first to document the existence of an association between climate and cholera outbreaks on the African continent, thus suggesting that cholera epidemics are also climate-linked in an epidemic context, and that there are consistent but nonstationary climatic effects on cholera incidence that can be observed across disparate landscapes and human communities, i.e., South America (Peru), Asia (Bangladesh), and Africa (Ghana).

A periodic common mode of fluctuation of 2–3 years for cholera time series cases and each of the five environmental parameters under scrutiny could be observed. Thus, when coherency was detected between time series, it occurred differently in time between pairwise comparisons: from 1989 to 1995 for cholera disease incidence and *IOI*; from 1988 to 1995 for incidence and rainfall, and incidence and *LSTA1*, respectively; from 1982 to 1995 for *LSTA1* and rainfall; from 1990 to 1995 for *LSTA1* and *IOI*; from 1989 to 1993 for rainfall and *IOI*; and, finally, from 1986 to 1992 between the two *LSTA* parameters.

Overall comparisons of the oscillating components demonstrated, during the time intervals for which there exists a covariation, that (i) the cholera case incidence and *IOI* shifted, with negative values of *IOI* having an advance of around 16 months on average over disease epidemics; (ii) cholera case incidences and rainfall were synchronous, with a very low time-lag (−0.75 months); (iii) disease incidence and *LSTA1* were out of phase, with *LSTA1* having an advance of around 6 months; (iv) *LSTA1* was in advance by around 6 months compared to rainfall (results not shown); and (v) *LSTA1* and *IOI* (with negative values corresponding to warm events) were also coherent but with a 12-month delay between warm events in tropical oceans and drought in Ghana, even though these associations appeared to be transient. Finally, the oscillating components computed for the two *LSTA* parameters showed that, from 1989 to 1993, these two temperature anomaly variables were more synchronous than in the previous time period.

Our work thus extends our understanding of the links between this environmentally persistent disease and climatic variability since it is for the first time focused on the area where the disease is the most prevalent, i.e., the West Africa. This global statistical interaction between cholera incidence cases and climate is a new and important informative finding, when reviewed in the context of recent publication of data for two other intertropical regions of the world, i.e., Asia and South America (Pascual et al., 2000, 2002; Rodo et al. 2002).

We observed that the onset of cholera epidemics in Ghana during the 1990s was highly correlated with previous warm events, as described by *LSTA1* and *LSTA2* parameters, which were clearly synchronous several months earlier. The influence of warm events, here quantified by the *LSTAs*, may indeed have an impact on the bacterial populations and that of their host reservoirs, providing new favorable environmental conditions such as an increase in temperature in shallow bodies of water, i.e., lagoons, estuaries, and coastal waters (Epstein, 1993; Salazar-Lindo et al., 1997; Checkley et al., 2000; Speelmon et al., 2000).

In addition, the influence of rainfall on cholera incidence, highlighted in this study by both coherency and oscillating component analyses which showed a time-lag of around 1 month between increased rainfall and cholera outbreaks in Ghana, can best be explained by the role of

flooding on disease transmission (Koelle et al., 2005b). However, this relationship between rainfall and cholera in Ghana needs to be explored with a more preciously dataset (e.g., weekly data), in order to clarify our result.

In addition, coherency and phase delay were detected between cholera incidence and both a global climate index (i.e., *IOI*) and local environmental parameters (i.e., *LSTA1* and *LSTA2*), which reinforce this hypothesis of an impact of climate on disease dynamics.

All of these findings suggest that it would be valuable to investigate additional cholera incidence time series in other parts of Africa and to compare these results with those already observed in western South America and the Bay of Bengal (Pascual et al., 2000, 2002; Speelmon et al., 2000; Rodo et al., 2002). With the observed impact of both global climate variability, and proximal environmental factors on cholera disease resurgence in human communities of Ghana, it is likely that populations across neighboring countries exhibit common temporal patterns of disease occurrence related to both lagged large-scale and lagged regional environmental variability. Because of the potentially complex interactions between climate, host reservoir abundance, human population densities, and cholera prevalence, it would be useful to determine whether similar trends in disease are observed between climate, on different scales, and cholera occurrence for other parts of the African continent. Other important socio-economic factors are undoubtedly important in explaining cholera prevalence and incidence (Faruque et al., 1998; Ali et al., 2002). Nevertheless, the search for correspondence across countries and regions of Africa in cholera outbreaks over time and their correlation with climatic factors should contribute to better understanding cholera dynamics. A variety of approaches is needed to tackle the disease in both epidemic and endemic contexts, in order to develop a predictive model, notably by monitoring the environment using remote sensing to protect public health. Indeed, previous investigations of cholera, in conjunction with the present study, suggest that knowledge of disease temporal and spatial patterns will help disentangle the intricate mechanisms behind the patterns observed.

Acknowledgments

This work was supported by a "Gestion et Impacts du Changement Climatique" grant (CHOLCLIM) from the French Ministry of Ecology and Sustainable Resources (FMESR). G.C.M. thanks the French authorities and the Centre National d'Etudes Spatiales (CNES) for PhD fellowships. B.C. is supported by the University Pierre & Marie Curie, Paris VI. J-F.G. thanks both the Institut de Recherche pour le Développement (IRD) and the Centre National de la Recherche Scientifique (CNRS).

References

Ali M, Emch M, Donnay JP, Yunus M, Sack RB (2002) The spatial epidemiology of cholera in an endemic area of Bangladesh. *Social Science & Medicine* 55:1015–1024

Bouma MJ, Pascual M (2001) Seasonal and interannual cycles of endemic cholera in Bengal 1891–1940 in relation to climate and geography. *Hydrobiologia* 460:147–156

Broutin H, Guégan J-F, Elguero E, Simondon F, Cazelles B (2005) Large-scale comparative analysis of pertussis population dynamics: periodicity, synchrony, and impact of vaccination. *American Journal of Epidemiology* 161:1159–1167

Cazelles B, Chavez M, McMichael AJ, Hales S (2005) Nonstationary influence of El Nino on the synchronous dengue epidemics in Thailand. *PLoS Medicine* 2:e106

Cazelles B, Stone L (2003) Detection of imperfect population synchrony in an uncertain world. *Journal of Animal Ecology* 72:953–968

Chatfield C (2004) *The Analysis of Time Series: an Introduction, 6th ed.*, Boca Raton, FL: Chapman & Hall/CRC

Checkley W, Epstein LD, Gilman RH, Figueroa D, Cama RI, Patz JA, et al. (2000) Effect of El Nino and ambient temperature on hospital admissions for diarrhoeal diseases in Peruvian children. *Lancet* 355:442–450

Colwell RR (1996) Global climate and infectious disease: the cholera paradigm. *Science* 274:2025–2031

Colwell RR, Huq A (2001) Marine ecosystems and cholera. *Hydrobiologia* 460:141–145

Colwell RR, Huq A, Islam MS, Aziz KM, Yunus M, Khan NH, et al. (2003) Reduction of cholera in Bangladeshi villages by simple filtration. *Proceedings of the National Academy of Sciences of the United States of America* 100(3):1051–1055

Epstein PR (1993) Algal blooms in the spread and persistence of cholera. *Biosystems* 31:209–221

Faruque SM, Albert MJ, Mekalanos JJ (1998) Epidemiology, genetics, and ecology of toxigenic *Vibrio cholerae*. *Microbiology and Molecular Biology Reviews* 62:1301–1314

Faruque SM, Naser IB, Islam MJ, Faruque AS, Ghosh AN, Nair GB, et al. (2005) Seasonal epidemics of cholera inversely correlate with the prevalence of environmental cholera phages. *Proceedings of the National Academy of Sciences of the United States of America* 102:1702–1707

Grenfell BT, Bjornstad ON, Kappey J (2001) Travelling waves and spatial hierarchies in measles epidemics. *Nature* 414:716–723

Islam MS, Drasar BS, Bradley DJ (1990) Long-term persistence of toxigenic *Vibrio cholerae* 01 in the mucilaginous sheath of a blue-green alga, *Anabaena variabilis*. *Journal of Tropical Medicine and Hygiene* 93:133–139

Islam MS, Drasar BS, Sack RB (1994) The aquatic flora and fauna as reservoirs of *Vibrio cholerae*: a review. *Journal of Diarrhoeal Diseases Research* 12:87–96

Islam MS, Rahim Z, Alam MJ, Begum S, Moniruzzaman SM, Umeda A, et al. (1999) Association of *Vibrio cholerae* O1 with the cyanobacterium, *Anabaena* sp., elucidated by polymerase chain reaction and transmission electron microscopy. *Transactions of Royal Society of Tropical Medicine and Hygiene* 93:36–40

Kelley L (2001) The global dimension of cholera. *Global Change & Human Health* 2:6–17

Koelle K, Pascual M, Yunus M (2005a) Pathogen adaptation to seasonal forcing, climate change. *Proceedings of the Royal Society of London. Series B: Biological Sciences* 272:971–977

Koelle K, Rodo X, Pascual M, Yunus M, Mostafa G (2005b) Refractory periods and climate forcing in cholera dynamics. *Nature* 436:696–700

Lipp EK, Huq A, Colwell RR (2002) Effects of global climate on infectious disease: the cholera model. *Clinical Microbiology Reviews* 15:757–770

Lobitz B, Beck L, Huq A, Wood B, Fuchs G, Faruque AS, et al. (2000) Climate and infectious disease: use of remote sensing for detection of *Vibrio cholerae* by indirect measurement. *Proceedings of the National Academy of Sciences of the United States of America* 97:1438–1443

Marsac F (2001) Climate and oceanographic indices appraising the environmental fluctuations in the Indian Ocean. *Indian Ocean Tuna Commission Proceedings* 4:293–301

Marsac F, Le Blanc JL (1998) Interannual and *ENSO*-associated variability of the coupled ocean-atmosphere system with possible impacts on the yellowfin tuna fisheries of the Indian and Atlantic oceans. *International Commission for the Conservation of Atlantic Tunas Collective Volume of Scientific Papers* 50:345–377

Miller CJ, Drasar BS, Feachem RG (1982) Cholera and estuarine salinity in Calcutta and London. *Lancet* 1:1216–1218

Montilla R, Chowdhury MA, Huq A, Xu B, Colwell RR (1996) Serogroup conversion of *Vibrio cholerae* non-O1 to *Vibrio cholerae* O1: effect of growth state of cells, temperature, and salinity. *Canadian Journal of Microbiology* 42:87–93

Pascual M, Bouma MJ, Dobson AP (2002) Cholera and climate: revisiting the quantitative evidence. *Microbes and Infection* 4:237–245

Pascual M, Rodo X, Ellner SP, Colwell R, Bouma MJ (2000) Cholera dynamics and El Nino-Southern Oscillation. *Science* 289:1766–1769

Piarroux R, Bompangue D (2006) Needs for an integrative approach of epidemics: the example of cholera. In: *Encyclopedia of Infectious Diseases: Modern Methodologies*, Tibayrenc M (editor), Chichester, UK: John Wiley & Sons Ltd (In press)

Rodo X, Pascual M, Fuchs G, Faruque AS (2002) *ENSO* and cholera: a nonstationary link related to climate change? *Proceedings of the National Academy of Sciences of the United States of America* 99:12901–12906

Salazar-Lindo E, Pinell-Salles P, Maruy A, Chea-Woo E (1997) El Nino and diarrhoea and dehydration in Lima, Peru. *Lancet* 350:1597–1598

Simanjuntak CH, Larasati W, Arjoso S, Putri M, Lesmana M, Oyofo BA, et al. (2001) Cholera in Indonesia in 1993–1999. *American Journal of Tropical Medicine and Hygiene* 65:788–797

Smith KF, Dobson AP, McKenzie FE, Real LA, Smith DL, Wilson ML (2005) Ecological theory to enhance infectious disease control and public health policy. *Frontiers in Ecology and the Environment* 3:29–37

Speelmon EC, Checkley W, Gilman RH, Patz J, Calderon M, Manga S (2000) Cholera incidence and El Nino-related higher ambient temperature. *JAMA* 283:3072–3074

Tamplin ML, Gauzens AL, Huq A, Sack DA, Colwell RR (1990) Attachment of *Vibrio cholerae* serogroup O1 to zooplankton and phytoplankton of Bangladesh waters. *Applied Environmental Microbiology* 56:1977–1980

Torrence C, Compo GP (1998) A practical guide to wavelet analysis. *Bulletin of the American Meteorological Society* 79:61–78

UNEP (2005) Emerging challenges—new findings. In: *Geo Year Book 2004–2005: an Overview of Our Changing Environment*, New York: United Nations Publications, pp 71–79

World Health Organization (2005) Cholera, 2004. *Weekly Epidemiological Record* 80:261–268

Xu H-S (1982) Survival and viability of non-culturable *Escherichia coli* and *Vibrio cholerae* in the estuarine and marine environment. *Microbial Ecology* 8:313–323